Experimental Improvements in Recording Gas-Phase Photoacoustic Spectra

Jan Davidsson, Jonathan H. Gutow, and Richard N. Zare*

Chemistry Department, Stanford University, Stanford, California 94305 *(Received: November 17, 1989)*

By adjusting several factors affecting the sensitivity of photoacoustic detection, we have constructed a general-purpose intracavity dye laser photoacoustic spectrometer with a detection limit of 4×10^{-10}/cm (2:1 signal-to-noise level). This permits small signals, such as the 4-0 and 5-0 O-H stretching bands of phenol, to be recorded in the gas phase at room temperature. It is found that the photoacoustic signal-to-noise ratio can be significantly enhanced by (1) reducing the effects of window absorption through the use of simple acoustic baffles and (2) the addition of a heavy rare gas as a sound carrier, changing the speed of sound and enabling a mechanical light chopper to modulate the light at an acoustic resonance frequency of the gas cell.

Introduction

Photoacoustic spectroscopy utilizes the fact that the absorption of light by a substance warms it, unless the energy is reemitted as light. If the light intensity is modulated, the temperature of the substance will oscillate. For an absorber that is in contact with or is a gas, the temperature oscillations cause periodic pressure variations—sound waves—which can be detected by a microphone or pressure gauge. The photoacoustic phenomenon was first reported by Bell in 1880.[1] There was little interest in photoacoustic spectroscopy until 1968 when Kerr and Atwood[2] used a laser as the light source.[3-5] With intense light sources photoacoustic detection is extremely sensitive because there is no heating of the gas if no light is absorbed, making the technique ideal for vibrational overtone spectroscopy[6] and trace gas analysis.[5]

Many factors affect the sensitivity of photoacoustic detection for a given absorptivity. The most basic is the intensity of the light source. As long as the transition of interest is not saturated, the sound intensity will increase linearly with the light intensity. The heat capacity of the sample, the inherent sensitivity of the microphone, the shape of the gas cell, and the light modulation frequency also affect the measured signal level. The major noise sources in a photoacoustic system are absorption at the windows, instabilities in the laser intensity, thermal noise in the microphones and electronics, and ambient noise in the laboratory, including physical motion of the sample cell.

In an attempt to improve the performance of our photoacoustic apparatus, we investigated several of the factors mentioned above. This study suggests many improvements. The two most important are (1) the use of simple acoustic baffles in the gas cell to reduce window noise and (2) the addition of a heavy rare gas to the sample, making it possible to modulate the light with a mechanical chopper at an acoustic resonance frequency of the gas cell. The improvements entail a new cell design, which is inexpensive, easy to maintain, has a relatively small internal volume, and is small enough to fit conveniently inside the cavity of a dye laser.

Experimental Section

The photoacoustic apparatus presented here is a significantly improved version of the ones previously used in this laboratory.[7,8] A block diagram of the apparatus is shown in Figure 1. We have two similar systems consisting of a linear dye laser pumped by an ion laser, whose output is mechanically modulated by a variable-speed chopper (Princeton Applied Research). We use 4-W all lines from an Ar^+ laser (Lexel 95) to pump R6G or DCM in one dye laser (Coherent 599 running broad band) and a Kr^+ laser (Spectra-Physics 171), producing 4-4.5-W multiline in the red, to pump LD700 in a second, home-built dye laser with the same optics geometry as the Coherent 599. In both dye lasers the output coupler is replaced with a flat high reflector of greater than 99% reflectivity in the region of interest. The unchopped intracavity power at the dye curve maximum is about 20 W for R6G and DCM and about 50 W for LD700. The lasers are tuned by rotating a three-plate birefringent filter using a stepping or gear motor. Our normal scan rate corresponds to about 20 cm^{-1}/min. The resolution of this system is about 1 cm^{-1}.

For the Coherent 599 laser it was necessary to extend the cavity to allow room for the sample cell. This entailed refocusing the folding mirror slightly to maintain stable operation. The proper focus is determined by adjusting the folding and back mirrors to give a constant beam diameter along the whole length of the laser cavity.

The photoacoustic signal from two battery-powered microphones (Knowles Electronics EA-3024) mounted in the cell are summed with a battery-powered home-built preamplifier. The preamplifier is based on a low-noise operational amplifier, either an OP-27 or an OP-37. We took great care to shield the amplifier and signal lines leading to it and increased the common mode rejection ratio by floating the microphone ground relative to the shield ground. The signal is then fed to a lock-in amplifier (PARC A-124) running in band-pass mode at the chopping frequency. Typically, the band-pass Q is set to 100 and the time constant to 300 ms for the scan rate given above. The phase is set on an intense peak in the spectrum before taking a scan of the spectrum and checked after the scan. As long as the chopper and lock-in amplifier are warmed up for at least 1 h, we do not see any drift in the phase.

The relative intracavity power is monitored with a photodiode connected to a lock-in (PARC HR-8) by collecting the reflection from one of the cell's Brewster angle windows; we have discussed some of the problems associated with this measurement of intracavity power previously.[8] The laser intensity transmitted through an etalon is measured by a photodiode and a lock-in (PARC 186A). A home-built variable-gain amplifier based on LF-356 operational amplifiers collects the laser-induced signal from a neon hollow cathode optogalvanic lamp.

All four signals are recorded independently by an IBM PC XT using a four-channel analog-to-digital converter with a resolution of about 2 mV out of a 10-V dynamic range. The etalon trace with a free spectral range of about 3.23 cm^{-1} and the optogalvanic lamp trace are used to make absolute frequency assignments with an accuracy of better than 0.5 cm^{-1}. The etalon traces are used to correct for the fact that the rotating birefringent filter does

(1) Bell, A. G. *Proc. Am. Assoc. Adv. Sci.* **1880**, *29*, 115.
(2) Kerr, E. L.; Atwood, J. G. *Appl. Opt.* **1968**, *7* (5), 915.
(3) Rosengren, L.-G. *Appl. Opt.* **1975**, *14* (8), 1960.
(4) Rosencwaig, A. Photoacoustics and Photoacoustic Spectroscopy. In *Chemical Analysis*; Elving, P. J., Winefordner, J. D., Eds.; Wiley: New York, 1980; Vol. 57.
(5) Zharov, V. P.; Letokhov, V. S. Laser Optoacoustic Spectroscopy. In *Springer Series in Optical Sciences*; Springer: Berlin, 1986; Vol. 37.
(6) Henry, B. R.; Sowa, M. G. *Prog. Anal. At. Spectrosc.* **1989**, *12* (4), 349.
(7) Chandler, D. W.; Farneth, W. E.; Zare, R. N. *J. Chem. Phys.* **1982**, *77*, 4447.
(8) Crofton, M. W.; Stevens, C. G.; Klenerman, D.; Gutow, J. H.; Zare, R. N. *J. Chem. Phys.* **1988**, *89*, 7100.

0022-3654/90/2094-4069$02.50/0

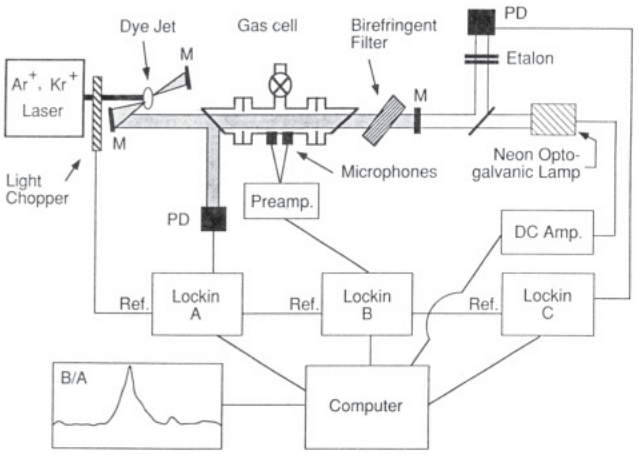

Figure 1. Dye laser photoacoustic spectrometer. PD, photodiode; M, laser mirror.

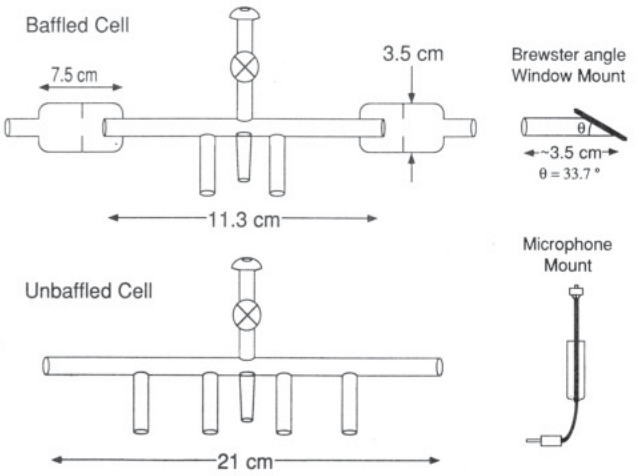

Figure 2. The two basic cell designs tested in this study. Microphones and window mounts are shown to the right. The finger at the center of each cell is for introducing samples or holding drying agents. The valves are Teflon with Viton O-ring seals. The figure is not to scale.

not scan completely linearly. The photoacoustic spectrum is the microphone signal divided by the relative intracavity power.

Two basic gas cell designs (Figure 2) were tested. The cells are made of Pyrex glass tubing with an i.d. near 6 mm. The first, a conventional overtone photoacoustic cell, consists of a tube with connections for up to four microphones and Brewster angle windows at each end. The second cell contains acoustic baffles to minimize window noise and accepts two microphones. Window and microphone mounts are attached to the cells with Cajon Ultra-Torr connectors. This makes it easy to replace dead microphones and dirty windows. The microphones and the 1-mm-thick fused silica windows (Dynatech Electro-Optics part HC0040SS) are glued to their respective mounts with epoxy (Figure 2).

The gas cells were evacuated on a glass vacuum line pumped by an oil diffusion pump. The typical base pressure in the line was 10^{-4} Torr. The vapor over solid phenol (Baker Analyzed Reagent Grade) at room temperature (~0.3 Torr[9]) was used as the sample because it provided a weak photoacoustic signal and a reproducible sample pressure. CaH_2 was mixed with the phenol in order to keep the gas sample dry and avoid interference from the strong water absorptions. The mixture was placed in a finger on the cell. Xenon, krypton, argon (Spectra Gases), or helium (Liquid Carbonic) of at least 99.99% purity was introduced as a buffer gas.

The fundamental vibrational spectrum of gas-phase phenol at room temperature was recorded on a Fourier transform infrared spectrometer (Bruker IFS 113), using a liquid-nitrogen-cooled HgCdTe (MCT) detector. The resolution of the spectrum was 2 cm^{-1}. An acquisition time of almost 1 h was needed (3200 scans). The sample cell was 15 cm long with NaCl windows. The identity of the phenol was verified by comparison with the gas-phase IR spectrum, taken in a GC study.[10]

Results and Discussion

The four factors we investigated that affect the sensitivity of photoacoustic detection are the sample molar heat capacity, the modulation frequency of the light, the noise produced at the windows of the cell, and the noise associated with the microphones and detection electronics. We discuss each of these in turn and then comment on their cumulative effect. As a demonstration of the improved sensitivity, we also present the gas-phase spectra of the phenol 4–0 and 5–0 O–H stretching overtones.

Heat Capacity. Consider the system to be a cell with constant volume. For an ideal gas

$$dT/dE = (nC_v)^{-1}$$

so that

$$dP/dE = R/(C_vV)$$

Here T is the temperature, P is the pressure, E is the absorbed energy, n is the number of moles of gas, C_v is the molar heat capacity at constant volume of the gas mixture, R is the gas constant, and V is the volume of the cell. For a real photoacoustic system the contents of the cell do not completely equilibrate at the modulation frequency; thus the equations above are a simplification. However, they do emphasize the basic constraints for maximizing the photoacoustic signal: (1) the gas mixture in the cell should have the lowest molar heat capacity possible, and (2) the effective volume of the cell should be as small as possible. The latter is also advantageous when the sample amount is limited.

The ideal conditions for photoacoustic spectroscopy are a gas mixture consisting of a small amount of sample buffered in a large amount of a nonabsorbing gas with a low C_v, such as rare gases, inside a cell with the smallest volume possible. Since the laser beam has cylindrical symmetry, the best way to minimize the volume is to use a cylindrically symmetric gas cell with an internal cell diameter barely larger than the diameter of the laser beam. To a first approximation, the absorption path length in the photoacoustic cell is unimportant. Inside the laser cavity the light intensity is constant along the beam length. This means that for a given absorptivity a constant amount of energy is absorbed per unit length and consequently increasing the path length in the cell does not increase the amount of energy absorbed per mole. However, for a resonant cell the length is important because it affects the frequency of acoustic resonances.

Microphones work poorly at low pressure, and a more detailed theoretical analysis suggests that the photoacoustic signal increases with increasing total pressure even if the absorber density is not increased.[2,3] However, we found that for our system the signal level was relatively constant for total pressures between 100 and 760 Torr. A total pressure of around 300 Torr worked well since the noise from outside of the cell seemed to be attenuated by the pressure mismatch.

We have used helium, krypton, and xenon as buffer gases and have not observed that there is a significant change in signal-to-noise ratio during nonresonant operation. However, there is a big advantage to buffering in a heavier gas as is discussed in the next section.

Acoustic Resonances. Acoustic resonances are a common phenomenon in enclosed spaces. However, calculating with reasonable accuracy the resonance frequencies of anything but the simplest of cell designs is difficult.[11,12] Cylindrical cells, without additions, such as baffles, gas valves, sample fingers, or microphone tubes, and which have a diameter of less than about

(9) Balson, E. W. *Trans. Faraday Soc.* **1947**, *43*, 48.

(10) Erickson, M. D.; Cooper, S. D.; Sparacino, C. M.; Zweidinger, R. A. *Appl. Spectrosc.* **1979**, *33* (6), 575.
(11) Nodov, E. *Appl. Opt.* **1978**, *17* (7), 1110.
(12) Bernegger, S.; Sigrist, M. W. *Appl. Phys. B* **1987**, *44* (2), 125.

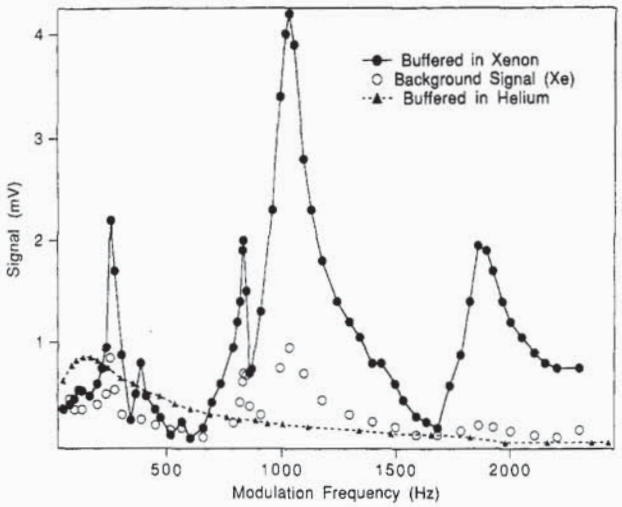

Figure 3. Photoacoustic signal versus modulation frequency. The phenol signal at 16 490 cm^{-1} with xenon or helium as buffer gas. Also shown is the background signal in xenon when the laser is tuned off the phenol band to about 16 350 cm^{-1}.

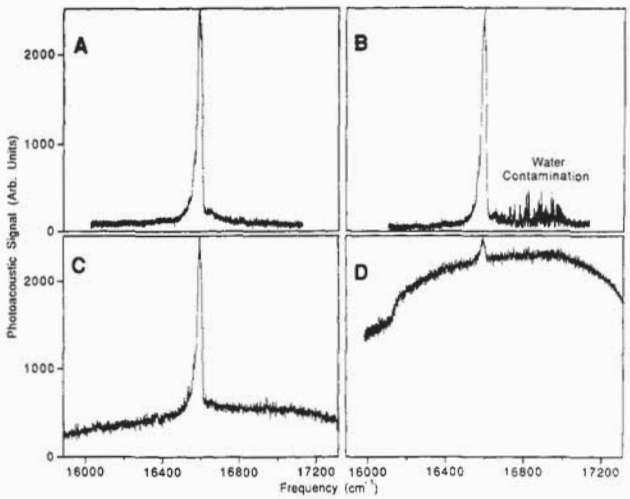

Figure 4. Phenol 5–0 O–H spectra: (A) clean windows on baffled cell; (B) clean windows on unbaffled cell; (C) dirty windows on baffled cell; (D) dirty windows on unbaffled cell. These spectra are *not* corrected for the variation of the laser intensity.

1/4 of a wavelength, behave as simple pipes. They display longitudinal resonances easily predicted by the following formula

$$f = cn/(2l) \qquad n = 1, 2, 3, \ldots$$

where c is the speed of sound in the gas within the tube, l is the length of the tube, and f is the resonance frequency. This formula is for an open-ended pipe or a pipe with both ends closed.[13] Since the speed of sound is inversely proportional to the mass density of the gas, the frequency is lower for a more massive gas. Consequently, the use of xenon instead of helium as a buffer makes it possible to construct a cell of reasonable length with resonance frequencies that are low enough to be accessible with a mechanical chopper.

The cell designs (Figure 2) tested in this study were used in both a resonant and nonresonant manner. In Figure 3 we show the signal intensity versus modulation frequency for our baffled cell with xenon or helium as the buffer gas. This chopping frequency scan was made by tuning the laser to the peak of the phenol absorption band at 16 490 cm^{-1} and then scanning the chopping frequency. The background level is the photoacoustic signal when the laser is tuned off of the gas absorption band ($\sim$16 350 cm^{-1}). For frequencies less than 300 Hz a chopper blade with fewer slits was used. The phase and gain of the lock-in was readjusted at each frequency. Note the dramatic variation of the signal intensity with chopping frequency. Although we do not show a chopping frequency scan for the unbaffled cell, it exhibits similar, but shifted, resonances.

The most important feature of Figure 3 is the enhancement of the signal level in the xenon buffered sample at about 1 kHz. This enhancement is caused by the first longitudinal acoustic resonance of the central pipe in the cell. Also seen are other smaller features reflecting additional acoustic modes of the cell. The assignment of the longitudinal resonance was verified by inserting a small glass tube into the cell, blocking the appendages. With this insert the central tube in the cell acts as a simple pipe, giving a somewhat simpler resonance pattern. We found that adding appendages does not affect the cell performance very much but increases the longitudinal frequencies by a small amount. Other possible types of resonances that might explain the more complicated pattern are Hemholtz, radial, and azimuthal; a more detailed discussion of these different types of resonances may be found elsewhere.[4,5,14,15] For comparison, the figure also contains a frequency scan for a helium-buffered sample. We are unable to mechanically modulate the light rapidly enough to reach a resonance. The increase of the signal intensity as the frequency decreases is a well-known phenomenon.[1,16]

For a photoacoustic spectrometer that is to be used for a large variety of samples the common approach has been to use small volume cells in a nonresonant manner.[6,16] In most cases the speed of sound varies among different gas mixtures, making it difficult to find or reach resonance frequencies. We buffer our samples in large amounts of rare gas; therefore, the heat capacity and the speed of sound are close to that in the pure rare gas. The speed of sound is effectively independent of the total buffer gas pressure. So it is relatively easy to search for the resonances after tuning the laser to an absorption. If, however, a large sample is necessary, a heavy buffer gas can still be used to lower the speed of sound and thus the resonance frequencies. In cases where the absorptions of interest are difficult to find, spiking the sample with a small amount of a stronger absorber facilitates determining the resonance frequency.

Lighter rare gases were tested. We found that krypton is also a suitable buffer gas. Buffering with krypton instead of xenon increases the resonance frequencies, but not beyond the limit of a mechanical chopper. Argon is too light for our cells; the main resonance frequency is too high. Replacing our mechanical chopper with, for instance, an acousto-optic modulator would remove this limitation. However, some work suggests that using the heavier noble gases as buffers increases the signal-to-noise level in acoustically resonant photoacoustic spectroscopy.[17] We have also seen indications of this.

Although working at resonance has many advantages, it does not significantly improve the signal-to-background ratio. This can be seen in Figure 3. The background level should not be confused with the random noise level. Most of the background arises from "window noise", discussed below. The advantage of operating resonantly is that the signal and background levels rise above the other noises in the system, such as ambient lab noise and electronic noise.[24]

"*Window Noise*". Small amounts of dirt or imperfections can cause heating at the windows and thus the production of a photoacoustic signal. Window absorption is a major problem for intracavity photoacoustic spectroscopy because of the high light intensity inside the cavity. The signature of window noise is that it is laser frequency independent; its intensity tracks the intensity of the exciting radiation. This signal can actually mask the signal

(13) Rossi, M. *Acoustics and Electroacoustics*; Artech House: Norwood, MA, 1988.
(14) *Optoacoustic Spectroscopy and Detection*; Pao, Y.-H., Ed.; Academic Press: New York, 1977.
(15) Nordhaus, O.; Pelzl, *J. Appl. Phys.* **1981**, *25*, 221.
(16) Wong, J. S. High Overtone Spectroscopy of Polyatomic Molecules. Doctoral Thesis, University of California, Berkeley, 1981 (available from University Microfilms International No. 8212153).
(17) Thomas, III, L. J.; Kelly, M. J.; Amer, N. M. *Appl. Phys. Lett.* **1978**, *32* (11), 736.

of interest[18] (see spectrum D in Figure 4). Rosengren[3] has shown that the window noise should decrease with increasing modulation frequency, which suggests that our relatively high modulation frequencies are advantageous. This is just discernible in Figure 3.

Our approach to this problem is to keep the windows as clean as possible and to place acoustic baffles between the windows and the body of the sample cell where the microphones are mounted. The latter is not a new idea; Zharov and Letokhov[5] have suggested a design similar to ours for pulsed photoacoustic spectroscopy. Our baffles do not decrease the signal level appreciably in contrast to higher Q, radially resonant systems where baffles decrease the quality of the resonances.[19]

The acoustic baffles can be seen in the side view of the baffled cell (Figure 2). The baffles hinder the propagation of the window noise into the central region of the cell near the microphones.[13] In an attempt to quantify the usefulness of the baffles, we collected the spectra shown in Figure 4. These spectra are the microphone signal, without ratioing to the intracavity power, versus laser frequency. For both the baffled and unbaffled cells we worked at the major longitudinal resonance frequency. From the figure it is immediately obvious how important it is to have clean windows. If the sample makes it difficult to keep the windows clean, a cell with baffles will perform much better than one without. Even with clean windows, the baffles give a flatter base line.

Electronic and Thermal Noise. The random noise level visible on the base lines of spectra A and B in Figure 4 is probably due to a combination of the ambient lab noise, noise from the microphones, associated electronics, and the fluctuations of the laser itself. The ultimate limit of a microphone's sensitivity is set by the random thermal fluctuations in the sample and of the microphone diaphragm.[5]

In practice, random fluctuations of the laser do not seem to be critical. Also, we measured the combined electronic noise of the lock-in, the preamplifier, and the FET amplifier in the microphones to be about 3 μV. This is at least a factor of 10 less than the noise level observed in the spectra. The noise, visible in the spectra, stems almost exclusively from thermal fluctuations and ambient lab noise. One of the major ambient noise sources is the mechanical chopper. In practice, this seems to set our detection limit. Acoustically isolating the chopper improves the noise, but replacing it with a nonmechanical modulator would be better since it also allows faster modulation.

In an attempt to reduce the effects of the microphone noise, we sum the output of two microphones in the low-noise preamplifier. Two microphones seem better than one when observing the noise level, but the difference is not as obvious in the spectra we have taken. However, the absolute signal level does increase with an increasing number of microphones; when the sample is weakly absorbing, more microphones are advantageous.

Implications. The improved version of our apparatus can detect a minimum absorptivity of 4×10^{-10}/cm with a signal-to-noise ratio of better than 2:1. This was verified by lowering the pressure of HD, which has overtones with well-known cross sections,[20] until a signal-to-noise ratio of 2:1 was achieved. The absorptivity corresponds to being able to detect 1 Torr of sample with a cross section of about 10^{-30} cm^2, localized in a bandwidth of about 1 cm^{-1}. For comparison, the limit of detectivity for a good Fourier transform infrared spectrometer is about 10^{-4} absorption units,[21] thus requiring a path length near 2500 m to measure an absorptivity of 4×10^{-10}/cm. Most commercial multipass White cells are available with maximum path lengths around 100 m. With our previous photoacoustic apparatus[8] we could detect a minimum absorptivity of 10^{-8}/cm, about a factor of 25 less than our present sensitivity.

It is interesting to compare our technique with more sophisticated ones. Deaton et al.[22] report a photoacoustic sensitivity of 10^{-10}/cm. They used a matched cell technique. Their CO_2 laser power was about 100 mW as compared with our 20–50 W. They were also using integration times of 1–10 min, which is 200–2000 times longer than ours. If we increase our integration times by this factor, theoretically, our sensitivity would be about 10^{-12}/cm. Assuming their background noise level would not rise in proportion to the laser intensity, at our laser powers they would have a detection limit of 10^{-12}–10^{-13}/cm. It is unclear whether their technique would perform this well, since the window noise must match in two cells.

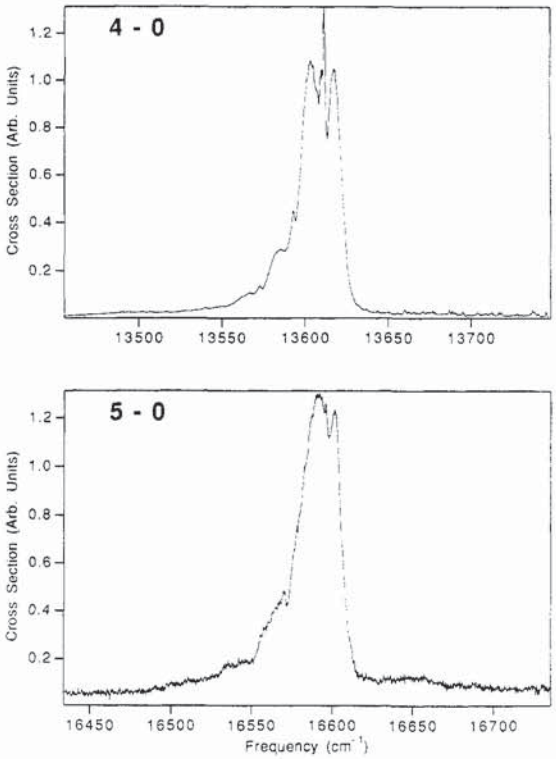

Figure 5. Gas-phase spectra of the 4–0 and 5–0 O–H stretching overtones of phenol, recorded at room temperature. These spectra are corrected for the variation of laser intensity.

TABLE I: Frequencies, Cross Sections, and Spectroscopic Parameters of the O–H Stretch of Gas-Phase Phenol

transition	freq, cm^{-1}	cross section, fm^2	spectroscopic parameters, cm^{-1}
1–0	3655	$(6.4 \pm 1.4) \times 10^4$	$\omega_0 = 3745$
4–0	13611	$(1.2 \pm 0.3) \times 10^1$	$\omega_0 = 88$
5–0	16490	1.4 ± 0.3	

Phenol Spectra. The room-temperature gas-phase overtone spectra of the 4–0 and 5–0 phenol O–H stretches are shown in Figure 5. Note that these spectra both show PQR structure. The O–H fundamental stretch was recorded with an FT-IR instrument. The quality of the fundamental spectrum was inferior to the overtone spectra, despite the fact that the overtone absorptions are 10^3–10^4 times weaker. Table I gives the band center frequencies, integrated cross sections, and the calculated Morse oscillator spectroscopic parameters. The latter are calculated by fitting to the expression $\nu = \omega_0 n + \omega_0 x_0 n^2$ where ν is the observed frequency, ω_0 is the harmonic frequency, $\omega_0 x_0$ is the anharmonicity, and n is the vibrational quantum number of the upper state.

The cross section for the overtones was estimated by comparison with the overtones of HD, as described by Gutow et al.[23] A phenol vapor pressure of 0.308 Torr was used for calculating the cross

(18) Gerlach, R.; Amer, N. M. *Appl. Phys.* **1980**, *23*, 319.
(19) Dewey, Jr., C. F. *Opt. Eng.* **1974**, *13*, 483.
(20) Trauger, J. T.; Mickelson, M. E. *Icarus* **1983**, *56*, 176.
(21) Buijs, H. In *Fourier Transform Infrared Spectroscopy*; Theophanides, T., Ed.; D. Reidel: Boston, 1984; p 43.
(22) Deaton, T. F.; Depatie, D. A.; Walker, T. W. *Appl. Phys. Lett.* **1975**, *26* (6), 300.
(23) Gutow, J. H.; Davidsson, J.; Zare, R. N. Unpublished work.
(24) Shtrikman, S.; Slatkine, M. *Appl. Phys. Lett.* **1977**, *31* (12), 830. Kritchman, E.; Shtrikman, S.; Slatkine, M. *J. Opt. Soc. Am.* **1978**, *68* (9), 1257.

sections.[9] The calculations assume that the phenol behaves as an ideal gas, possibly underestimating the number density and yielding too large a cross section.

Conclusion

We have demonstrated a photoacoustic apparatus and technique capable of detecting a minimum absorptivity on the order of 4×10^{-10}/cm. To demonstrate this sensitivity, we recorded the 4–0 and 5–0 O–H overtone spectra of phenol in the gas phase using the vapor present over the solid at room temperature. Several modifications to the standard methods of overtone photoacoustic spectroscopy were made to achieve this level of sensitivity. Two important and simple changes are that the cell is run at an acoustic resonance with a heavy rare gas as a buffer and that baffles are added between the windows and the region near the microphone. Although the cell design described in this paper is not necessarily optimal, we believe that it offers many advantages for intracavity gas-phase photoacoustic spectroscopy because the design is simple, inexpensive, easy to maintain, may be used for a wide variety of samples, even those with limited vapor pressure, and is still extremely sensitive.

Acknowledgment. We thank Jan Van Gastel, our departmental glassblower, for making and remaking our cells for us. J.D. received his support from the Swedish Natural Research Council. This work was supported by NSF Grant CHE 85-05926.

Ground-State Dimers in Excimer-Forming Bichromophoric Molecules. NMR and Single-Photon-Counting Data. 2. Racemic and Meso Dipyrenylpentanes and Dipyrenylalkanes

Peter Reynders,† Wolfgang Kühnle, and Klaas A. Zachariasse*

Max-Planck-Institut für biophysikalische Chemie, Abteilung Spektroskopie, Postfach 2841, Am Fassberg, D-3400 Göttingen, Federal Republic of Germany *(Received: January 3, 1990)*

^{1}H NMR spectra of the racemic and meso diastereomers of 2,4-di(1-pyrenyl)pentane (1DPP) in toluene-d_8 and of the 1,*n*-di(1-pyrenyl)alkanes (1Py(*n*)1Py with $n = 0$–10 and 13) and 1,*n*-di(2-pyrenyl)alkanes (2Py(*n*)2Py with $n = 1$–10 and 14) in chloroform-*d* were measured at room temperature. The conformer distribution in both 1DPP molecules was determined from an analysis of the vicinal coupling constants between the methylene and methine protons. In *meso*-1DPP, an intramolecular sandwichlike ground-state dimer was detected, whereas in *rac*-1DPP a dimer only overlapping at the aromatic protons H9 and H10 is formed. The presence of both dimers was confirmed by time-resolved fluorescence measurements (single-photon counting (SPC)). With the dipyrenylalkanes, an analysis of the chemical shifts of the aromatic protons shows that sandwich dimers are not present. Only in the case of 1Py(3)1Py is a partial-overlap dimer detected. These findings are supported by results from SPC measurements.

Introduction

Intramolecular excimer formation has been studied with various dipyrenylalkanes,[1-5] including meso and racemic dipyrenylpentanes,[2,3] by employing photostationary and time-resolved fluorescence measurements. With 1,3-di(2-pyrenyl)propane, 2Py(3)2Py, it has been shown that the monomer and excimer fluorescence decays are double-exponential,[4] whereas triple-exponential decays were observed in the case of 1,3-di(1-pyrenyl)propane, 1Py(3)1Py.[1d,5] These data have been analyzed by use of a kinetic scheme consisting of two or three discrete excited states, respectively, identified as one group of rapidly (<400 ps) interconverting monomer conformers and either one or two excimers.[3-5] In a different approach, the monomer fluorescence decays of 1Py(3)1Py have been interpreted by using distributions of decay times.[5b,6] As ground-state dimers have been detected in both series of the 1,*n*-bis(1-pyrenylcarboxy)- and 1,*n*-bis(2-pyrenylcarboxy)alkanes,[7] leading to changes in the kinetic schemes and hence in the treatment of data coming from the fluorescence experiments,[3b] the presence of dimers was also investigated for the corresponding dipyrenylalkanes. The results of these studies, comprising ^{1}H NMR and time-correlated single-photon-counting (SPC) measurements, are reported in this paper.

Experimental Section

1,6-Di(1-pyrenyl)hexane,[8] 1Py(6)1Py, was synthesized as follows. 6-(1-Pyrenyl)hexanoic acid (mp 200–201 °C) was made from the monoethyl ester of 1,6-hexanedioic acid chloride in a Friedel–Crafts reaction with pyrene and subsequent reduction with hydrazine hydrate. The acid chloride of this compound was reacted with pyrene to 1-(1-pyrenoyl)-5-(1-pyrenyl)pentane (mp 172–174 °C), which was reduced (Huang–Minlon) to 1Py(6)1Py (mp 187–188 °C). The synthesis of the other compounds treated here has been described before[1a,3b,4] or will be published elsewhere.

* Correspondence and reprint requests may be addressed to this author.
† Present address: AT&T Bell Laboratories, Murray Hill, NJ 07974-2070.

(1) (a) Zachariasse, K. A.; Kühnle, W. *Z. Phys. Chem.* **1976**, *101*, 267. (b) Zachariasse, K. A.; Kühnle, W.; Weller, A. *Chem. Phys. Lett.* **1978**, *59*, 375. (c) Snare, M. J.; Thistlethwaite, P. J.; Ghiggino, K. P. *J. Am. Chem. Soc.* **1983**, *105*, 3328. (d) Zachariasse, K. A.; Duveneck, G.; Busse, R. *J. Am. Chem. Soc.* **1984**, *106*, 1045. (e) Anderson, V. C.; Craig, B. B.; Weiss, R. G. *J. Am. Chem. Soc.* **1984**, *106*, 6628. (f) Sonnenschein, M. F.; Weiss, R. G. *J. Phys. Chem.* **1988**, *92*, 6828. (g) Zachariasse, K. A. In *Photochemistry on Solid Surfaces*; Matsuura, T., Anpo, M., Eds.; Elsevier: Amsterdam, 1989; p 48.

(2) (a) Collart, P.; Toppet, S.; Zhou, Q. F.; Boens, N.; De Schryver, F. C. *Macromolecules* **1985**, *18*, 1026. (b) Collart, P.; Toppet, S.; De Schryver, F. C. *Macromolecules* **1987**, *20*, 1266.

(3) (a) Zachariasse, K. A.; Duveneck, G.; Kühnle, W.; Reynders, P.; Striker, G. *Chem. Phys. Lett.* **1987**, *133*, 390. (b) Reynders, P.; Dreeskamp, H.; Kühnle, W.; Zachariasse, K. A. *J. Phys. Chem.* **1987**, *91*, 3982. (c) Reynders, P. Ph.D. Thesis, Göttingen University, 1988.

(4) Zachariasse, K. A.; Duveneck, G.; Kühnle, W. *Chem. Phys. Lett.* **1985**, *113*, 337.

(5) (a) Zachariasse, K. A.; Busse, R.; Duveneck, G.; Kühnle, W. *J. Photochem.* **1985**, *28*, 237. (b) Zachariasse, K. A.; Striker, G. *Chem. Phys. Lett.* **1988**, *145*, 251. (c) Zachariasse, K. A.; Busse, R.; Duveneck, G.; Kühnle, W. In *Excited State Probes in Biochemistry and Biology*; Szabo, A., Ed.; Plenum: New York, in press. (d) Zachariasse, K. A.; Busse, R. In *Excited State Probes in Biochemistry and Biology*; Szabo, A., Ed.; Plenum: New York, in press.

(6) Siemiarczuk, A.; Ware, W. R. *Chem. Phys. Lett.* **1987**, *140*, 277.

(7) Reynders, P.; Kühnle, W.; Zachariasse, K. A. *J. Am. Chem. Soc.* **1990**, *112*, 3929.

(8) The compound presented as 1Py(6)1Py in ref 1a was $1PyCH_2CH(CH_3)(CH_2)_31Py$; see ref 5c. Professor R. G. Weiss is thanked for drawing our attention to this problem.

0022-3654/90/2094-4073$02.50/0